Cancer Cell
Article

A Molecule Targeting VHL-Deficient Renal Cell Carcinoma that Induces Autophagy

Sandra Turcotte,[1] Denise A. Chan,[1] Patrick D. Sutphin,[1] Michael P. Hay,[2] William A. Denny,[2] and Amato J. Giaccia[1,*]
[1]Department of Radiation Oncology, Stanford University School of Medicine, Stanford, CA 94305, USA
[2]Auckland Cancer Society Research Centre, The University of Auckland, Private Bag 92019, Auckland 1142, New Zealand
*Correspondence: giaccia@stanford.edu
DOI 10.1016/j.ccr.2008.06.004

SUMMARY

Renal cell carcinomas (RCCs) are refractory to standard therapies. The von Hippel-Lindau (*VHL*) tumor suppressor gene is inactivated in 75% of RCCs. By screening for small molecules selectively targeting VHL-deficient RCC cells, we identified STF-62247. STF-62247 induces cytotoxicity and reduces tumor growth of VHL-deficient RCC cells compared to genetically matched cells with wild-type VHL. STF-62247-stimulated toxicity occurs in a HIF-independent manner through autophagy. Reduction of protein levels of essential autophagy pathway components reduces sensitivity of VHL-deficient cells to STF-62247. Using a yeast deletion pool, we show that loss of proteins involved in Golgi trafficking increases killing by STF-62247. Thus, we have found a small molecule that selectively induces cell death in VHL-deficient cells, representing a paradigm shift for targeted therapy.

INTRODUCTION

Mutations and/or inactivation of the von Hippel-Lindau (*VHL*) tumor suppressor gene occur in the majority of renal cell carcinomas (RCCs) of the clear cell phenotype. Restoration of VHL function in $VHL^{-/-}$ RCCs results in significant inhibition of tumor formation by these cells in nude mice, demonstrating the tumor suppressor function of VHL (Iliopoulos et al., 1995). Functional studies indicate that pVHL, the protein product of *VHL*, is an E3 ubiquitin ligase that targets the α subunit of the hypoxia-inducible factor (HIF) for proteasomal degradation under normoxia. In the presence of oxygen, hydroxylation on proline residues 564 and 402 by prolyl hydroxylases (PHDs) marks HIF-α for recognition and binding with pVHL, leading to degradation of HIF-α. Under hypoxic conditions, activity of the PHDs decreases, reducing recognition of HIF-α by pVHL (Chan et al., 2002; Ivan et al., 2001; Jaakkola et al., 2001). In cells that lack VHL, stabilized HIF-α binds constitutively expressed HIF-β to activate the transcription of genes involved in metabolism, angiogenesis, invasion and metastasis, and proliferation (Erler et al., 2006; Gnarra et al., 1996; Iliopoulos et al., 1996; Knebelmann et al., 1998; Staller et al., 2003). In addition to its role in HIF regulation, pVHL has been implicated in a variety of HIF-independent processes including extracellular matrix assembly, regulation of microtubule stability, polyubiquitination of atypical protein kinase C (PKC) family members, regulation of fibronectin, and modulation of RNA polymerase II subunits (Hergovich et al., 2003; Na et al., 2003; Ohh et al., 1998; Okuda et al., 2001). It has also been reported that an acidic domain present in the N-terminal region of pVHL contributes to its tumor suppressor function in a HIF-independent manner and may be relevant for the development of VHL-associated malignancies (Lolkema et al., 2005).

Defects in apoptosis that are observed in many solid tumor cells, including RCCs, increase the resistance of tumor cells to chemotherapy, radiotherapy, and molecularly targeted therapies. In contrast to apoptosis, autophagy regulates the turnover of organelles and long-lived proteins to ensure homeostasis. Under metabolic stress, autophagy is activated and promotes survival (Mathew et al., 2007). In some cell types, autophagy can also result in cell death under persistent stress conditions. Studies have reported a dysregulated level of autophagy in diverse diseases including neuronal degeneration, infectious

SIGNIFICANCE

Inactivation of the von Hippel-Lindau (*VHL*) tumor suppressor gene arises in the majority of renal cell carcinomas (RCCs) and is associated with a high degree of vascularization and poor prognosis. We evaluated the possibility of targeting VHL-deficient cells through a synthetic lethality approach by screening for small molecules that exhibit toxicity to renal cells lacking *VHL*. We identified a compound, STF-62247, which was selectively cytotoxic toward VHL-deficient cells in vitro and in vivo. We demonstrate that STF-62247 induces autophagy and that inhibition of autophagy significantly reduces sensitivity to STF-62247. Since RCCs are refractory to standard cytotoxic chemotherapies, there is a need for additional chemotherapies. STF-62247 is a small molecule that exploits the loss of *VHL* in RCC.

disease, and cancer (Kondo et al., 2005). Whether autophagy protects against or causes these diseases is still unclear, but the regulation of autophagy has promising therapeutic implications.

Autophagy occurs in all eukaryotic cells from yeast to mammals. In response to a diverse number of stimuli such as starvation, hypoxia, or high temperature, portions of cytoplasm and organelles are sequestered in a double-membrane vesicle called an autophagosome. These vesicles undergo maturation by fusion with endosomes and/or lysosomes to become autolysosomes, whose contents are degraded by hydrolases (Klionsky and Emr, 2000). Among autophagy-related genes (ATGs) identified to regulate this process, beclin 1 (*BECN*), the mammalian ortholog of yeast *ATG6*, acts as a tumor suppressor gene in mice and is frequently deleted in human cancers (Aita et al., 1999). In mammalian cells, *BECN* forms a complex with the class III family of phosphatidylinositol 3-kinases (PI3Ks) and localizes at the trans-Golgi network (TGN) (Kihara et al., 2001). The elongation of the double membrane involves two ubiquitin-like conjugation systems: the ATG5-ATG12 complex and the microtubule-associated protein light chain 3 (MAP-LC3; *ATG8* in yeast). In unstressed cells, LC3 is present in the cytoplasm, while the lipidated form of LC3 is associated with double-membrane-containing organelles in cells undergoing autophagy (Kabeya et al., 2000). The recruitment of LC3 to the membrane occurs in an *ATG5*-dependent manner. While ATG5-ATG12 dissociate from the membrane upon completion of autophagosome formation, LC3 remains associated with the membrane (Kabeya et al., 2000; Mizushima et al., 2001). ATG7 acts as an E1 enzyme in the autophagy conjugation system, where, in combination with an E2 enzyme, it conjugates phosphatidylethanolamine to LC3-I to form LC3-II, and no lipidation of LC3 occurs in the brain of *Atg7*-deficient mice (Tanida et al., 2002). On the other hand, ATG9 has been reported to cycle between the TGN and endosomes, and its disruption impairs formation of autophagosomes (Young et al., 2006).

Cell-based small-molecule screening has been used to identify compounds that inhibit specific proteins, such as HIF, or to overcome drug resistance to reduce tumorigenicity (Isaacs et al., 2002; Mabjeesh et al., 2003; Rapisarda et al., 2002; Smukste et al., 2006). In this report, we describe a small molecule identified from a screen, STF-62247, that induces autophagy and selectively induces lethality in RCCs that have lost the *VHL* tumor suppressor gene. We further use a yeast deletion pool to functionally investigate the targets of STF-62247 that are involved in cell killing.

RESULTS

STF-62247 Induces Cytotoxicity and Reduces Tumor Growth in VHL-Deficient Cells in a HIF-Independent Manner

In this study, we evaluated the possibility of selectively targeting VHL-deficient cells using small-molecule compounds. We screened 64,000 compounds against wild-type VHL and VHL-deficient RCCs (unpublished data) that were stably transfected with enhanced yellow fluorescent protein (EYFP). The effect of small molecules on each cell type was monitored separately by fluorescence (Figure 1A). The drug STF-62247 was identified in this screen (see Figure S1A available online) and decreased the viability of VHL-deficient cells in a short-term assay (Figure S1B). Moreover, STF-62247 specifically results in cytotoxicity in renal cells that have lost VHL as demonstrated using two genetic models: VHL-deficient RCC4 cells and their counterparts that express ectopically introduced wild-type VHL, and VHL-proficient SN12C cells and their counterparts that stably express shRNA targeting VHL (Thomas et al., 2006). Clonogenic assays demonstrated that STF-62247 is selectively toxic to VHL-deficient cells compared to their wild-type VHL counterparts (Figure 1B).

Since VHL is an important negative regulator of HIF-α through its E3 ligase activity, we used *VHL*-null RCC4 cells expressing shRNA against HIF-1α or HIF-2α to determine whether STF-62247 cytotoxicity is dependent on HIF (Figure 1C, bottom panel). The level of HIF target genes was quantified by qRT-PCR, verifying functional knockdown of HIF (Figure S1C). Clonogenic assays demonstrated that the reduction of either HIF-1α or HIF-2α in *VHL*-null cells did not affect cell death induced by STF-62247 (Figure 1C, upper panel). Also, decreasing the level of ARNT (HIF-1β) using shRNA did not change the cell sensitivity to STF-62247 (data not shown). Previous studies have indicated that HIF-2 is critical for tumor growth of RCCs (Kondo et al., 2003; Zimmer et al., 2004). To further investigate the effect of HIF-2 in the sensitivity of RCC4 cells to STF-62247, we generated a VHL cell line that stably expressed a normoxically stable, constitutively active HIF-2α mutant, P531A N847A. Two individual HIF-2α RCC4/VHL clones were randomly chosen that had elevated HIF-2α expression under normoxic conditions (Figure 1D, bottom panel). The results show that cytotoxicity of STF-62247 was unaffected by the presence of HIF-2α expression under normoxic conditions when compared to RCC4/VHL cells. Thus, by using complementary approaches, our results indicate that STF-62247 induces cytotoxicity in *VHL*-null cells in a HIF-independent manner.

To evaluate the effect of STF-62247 on tumor growth in vivo, we implanted SN12C, SN12C-VHL shRNA, or 786-O cells subcutaneously into the flanks of immunodeficient mice. The selective cytotoxicity of STF-62247 for the VHL-deficient cells was also demonstrated in 786-O cells compared to their wild-type VHL counterparts by clonogenic assay in vitro (Figure S1D). Daily treatment with STF-62247 significantly reduced tumor growth of VHL-deficient cells (Figure 1E). This decrease in tumor growth was concentration dependent. Importantly, drug treatment did not have any effect on the growth of SN12C tumor cells that have wild-type VHL (Figure S1E). Together, these results show that STF-62247 selectively kills RCC cells with a loss of VHL in vitro and also significantly reduces tumor growth in cells deficient in VHL.

Autophagy Is Induced by STF-62247 Treatment

We found that STF-62247 did not induce apoptosis in vitro in VHL-deficient cells as assayed by Hoechst staining (Figure S1F), annexin V staining (Figure S1G), or caspase-3 immunoblot (Figure S1H). These results were further confirmed by immunostaining for caspase-3 in tumor sections (Figure S1I). There was no difference in proliferation as assayed by Ki67 staining in response to STF-62247 in RCCs deficient in VHL or with wild-type VHL (Figure S1J). STF-62247 did not induce DNA

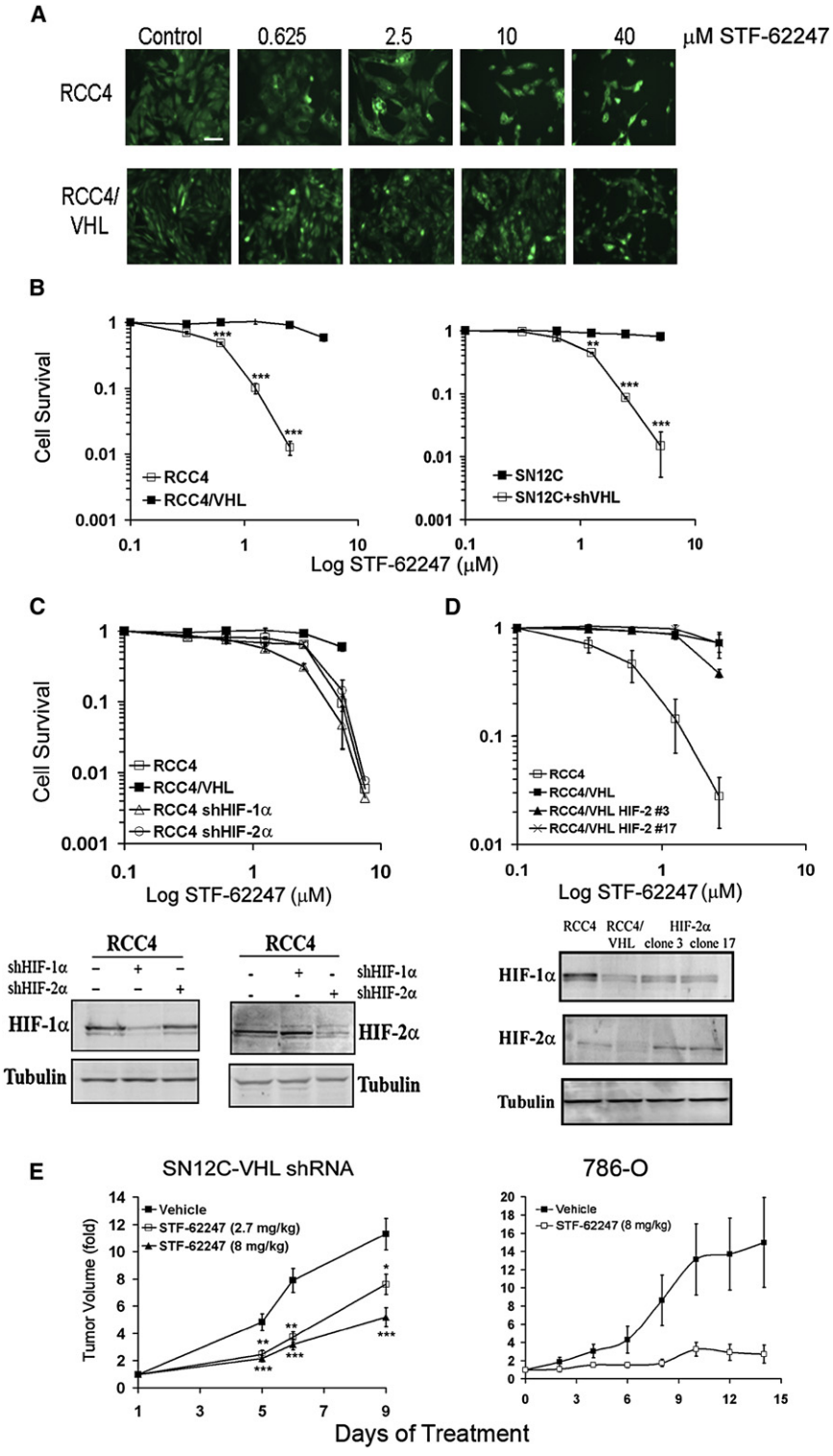

Figure 1. STF-62247 Induces Cytotoxicity and Reduces Tumor Growth in VHL-Deficient Cells in a HIF-Independent Manner

(A) RCC4 and RCC4/VHL cells were labeled with enhanced yellow fluorescent protein (EYFP) and treated with increasing concentration of STF-62247 for 4 days. Each cell type was monitored by fluorescence separately. Cells are pseudocolored green. Scale bar = 10 μm.

(B) Clonogenic assay in RCC4, RCC4/VHL, SN12C, and SN12C-VHL shRNA cells in the presence of STF-62247 (0–30 μM). Each point of cell survival is calculated by the average of three different experiments in triplicate as the percent of treated on untreated plate.

(C) Upper panel: clonogenic assay for RCC4 cells infected with HIF-1α or HIF-2α shRNA by retroviral infection in presence of drug in the same conditions described above. Lower panel: HIF-1α or HIF-2α protein expression evaluated by western blot in RCC4 cells with HIF-1α or HIF-2α shRNA. Tubulin was used as loading control.

(D) Upper panel: clonogenic assay with STF-62247 in VHL-positive RCC4 cells where HIF-2α was stably introduced by retroviral infection. Lower panel: western blot for HIF-1α or HIF-2α in VHL-positive RCC4 cells.

(E) SN12C-VHL shRNA cells (2–3 × 10^6) and 786-O cells (5 × 10^6) were injected into SCID mice. SN12C-VHL tumor-bearing mice were treated daily with vehicle or with 2.7 mg/kg or 8 mg/kg STF-62247 by intraperitoneal injection. 786-O tumor-bearing mice were treated with vehicle or 8 mg/kg STF-62247. Five tumors per condition were analyzed. *$p < 0.05$, **$p < 0.01$, ***$p < 0.005$. All error bars represent standard error of the mean (SEM).

damage as measured by the comet assay (data not shown). In addition, phosphorylation of p53 on serine 15 and total p53 levels were unaffected by STF-62247 treatment, further supporting the lack of a DNA damage signal in cell killing induced by STF-62247 (Figure S1K). We observed that STF-62247-treated cells accumulated intracytoplasmic vacuoles characteristic of cells undergoing autophagy. Moreover, these vacuoles were larger in VHL-deficient RCC4 and SN12C-VHL shRNA cells than in wild-type VHL cells (Figure 2A). Vacuole formation in RCC cells with and without VHL was monitored by time-lapse microscopy for 48 hr, which showed that vacuoles appear as soon as 3 hr after adding STF-62247 (Movies S1 and S2). The time-lapse movies also indicate that wild-type VHL prevents the formation of larger vacuoles present in VHL-deficient cells.

Induction of autophagy was confirmed by immunostaining and western blotting for LC3. STF-62247 increased punctate staining of LC3, which is associated with processing of LC3 to its lipidated form (Figure 2B). LC3-II, corresponding to the lipidated form found with the formation of double membranes, was induced by STF-62247 treatment, indicating that STF-62247 stimulates autophagy (Figure 2D). Transmission electron microscopy was also used to monitor autophagy in response to STF-62247. There were large numbers of autophagic vacuoles present in

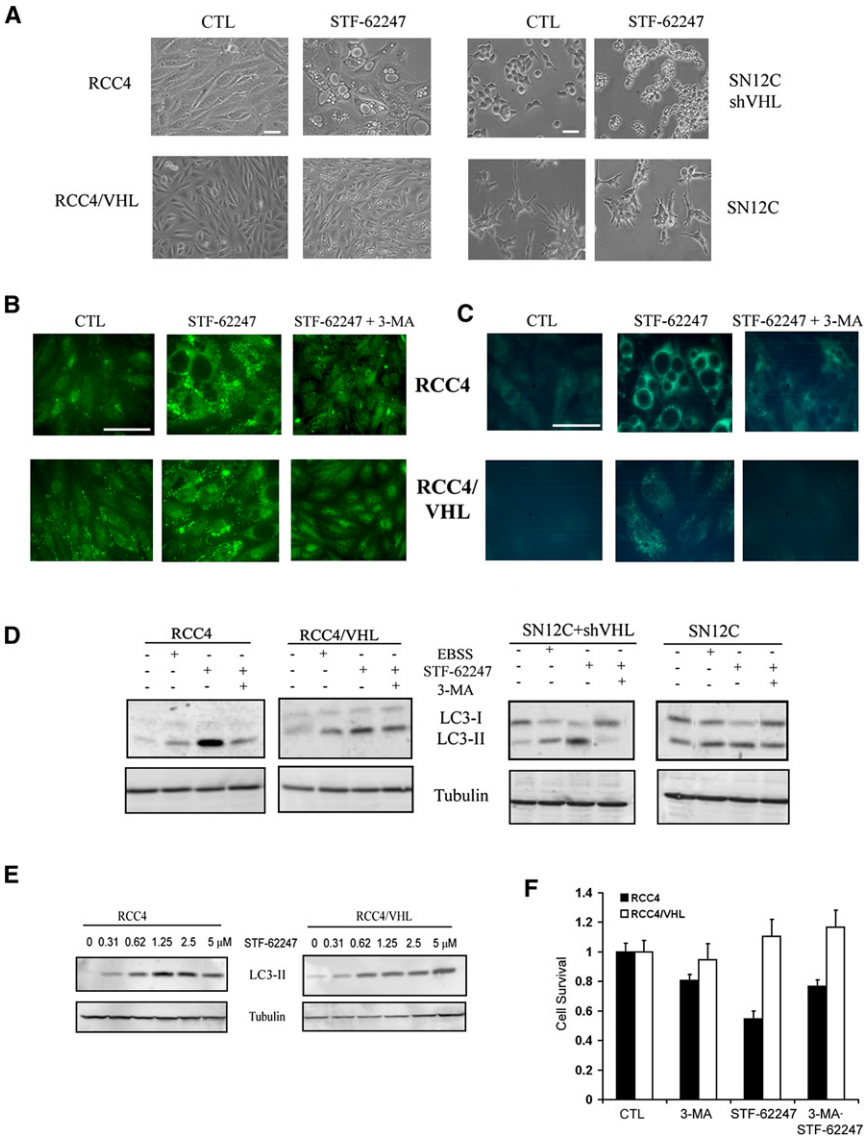

Figure 2. Presence of Autophagic Vacuoles with STF-62247 in Renal Cell Carcinomas

(A) Phase-contrast images of VHL-deficient RCC4 and SN12C-VHL shRNA cells (top) and VHL-positive RCC4 and SN12C cells (bottom) after 20 hr of treatment with 1.25 μM STF-62247.

(B) Immunostaining for LC3 following 1.25 μM STF-62247 treatment for 20 hr with or without 2 mM 3-methyladenine (3-MA) in RCC4 cells with and without VHL. After treatment, cells were fixed, permeabilized, and processed for detection of punctate staining by indirect immunofluorescence.

(C) Autophagic vacuoles stained with monodansylcadaverine (MDC). After STF-62247 treatment under the same conditions, MDC was added for the final 10 min. Cells were fixed, washed with PBS, and observed directly under a microscope.

(D) Western blot for LC3 in RCC4, RCC4/VHL, SN12C-VHL shRNA, and SN12C cells after STF-62247 treatment with or without 3-MA. Nutrient starvation (EBSS) was used as positive control.

(E) Western blot for LC3 in RCC4 and RCC4/VHL cells with different concentrations of STF-62247. Tubulin was used as loading control.

(F) Cell viability assay in VHL-deficient RCC4 and wild-type VHL cells treated with 1 mM 3-MA, 1.25 μM STF-62247, or both for 24 hr. Viability was measured by trypan blue exclusion assay and is represented by the average of three different experiments in duplicate as the percent of treated on untreated cells. Error bars represent SEM.

All scale bars = 10 μm.

STF-62247-treated cells, but not in untreated cells (Figure S2A). The presence of double-membrane-containing cellular organelles was observed in treated RCC4 cells at higher magnification (Figure S2B).

The increase of the LC3-II form was abrogated by 3-methyladenine (3-MA), an autophagy inhibitor that inhibits PI3K. It is noteworthy that although the stimulation in LC3 was higher in VHL-deficient cells treated with STF-62247, the increase was also observed in wild-type VHL cells, and therefore the presence of autophagosomes cannot by itself explain the difference in toxicity observed between RCC cells with and without VHL. We also stained cells with the autofluorescent compound monodansylcadaverine (MDC), which acts as a lysosomotropic agent and labels some of the acidic compartments that are observed after fusion with lysosomes (autolysosomes) (Figure 2C). Staining with MDC in RCC4 cells was primarily observed around the larger vacuoles compared to the punctate staining of LC3, suggesting that these large vacuoles are associated with the acidic components of autolysosomes.

Since autophagy might be an early response during drug treatment, LC3 processing was monitored in cells exposed to increasing concentrations of drug. The results show that the LC3-lipidated form increased in a concentration-dependent manner, indicating that the autophagic process is tightly linked with drug cytotoxicity (Figure 2E). To determine whether autophagy induced by STF-62247 was responsible for the reduced viability observed in VHL-deficient cells, we measured the viability after 24 hr of cells treated with 3-MA to inhibit autophagy. The viability of VHL-deficient cells was partially restored by 3-MA, indicating that STF-62247-induced autophagy leads to cell death in VHL-deficient cells (Figure 2F).

ATG5, ATG7, and ATG9 Are Involved in Autophagosome Formation in STF-62247-Treated Cells

We hypothesized that if autophagy is important in STF-62247 cytotoxicity of VHL-deficient cells, *Atg5*$^{-/-}$ cells would be less sensitive to STF-62247-induced cell death. We found significantly more autophagic vacuoles during STF-62247 treatment in *Atg5*$^{+/+}$ cells compared to *Atg5*$^{-/-}$ cells (Figure 3A). This effect correlates with the LC3 processing that was observed only in *Atg5*$^{+/+}$ cells in response to STF-62247 and was concentration dependent (Figure 3B). Importantly, we confirmed that *ATG5* is involved in STF-62247-induced toxicity in VHL-deficient RCC cells. Silencing *ATG5* in VHL-deficient RCC4 cells by siRNA

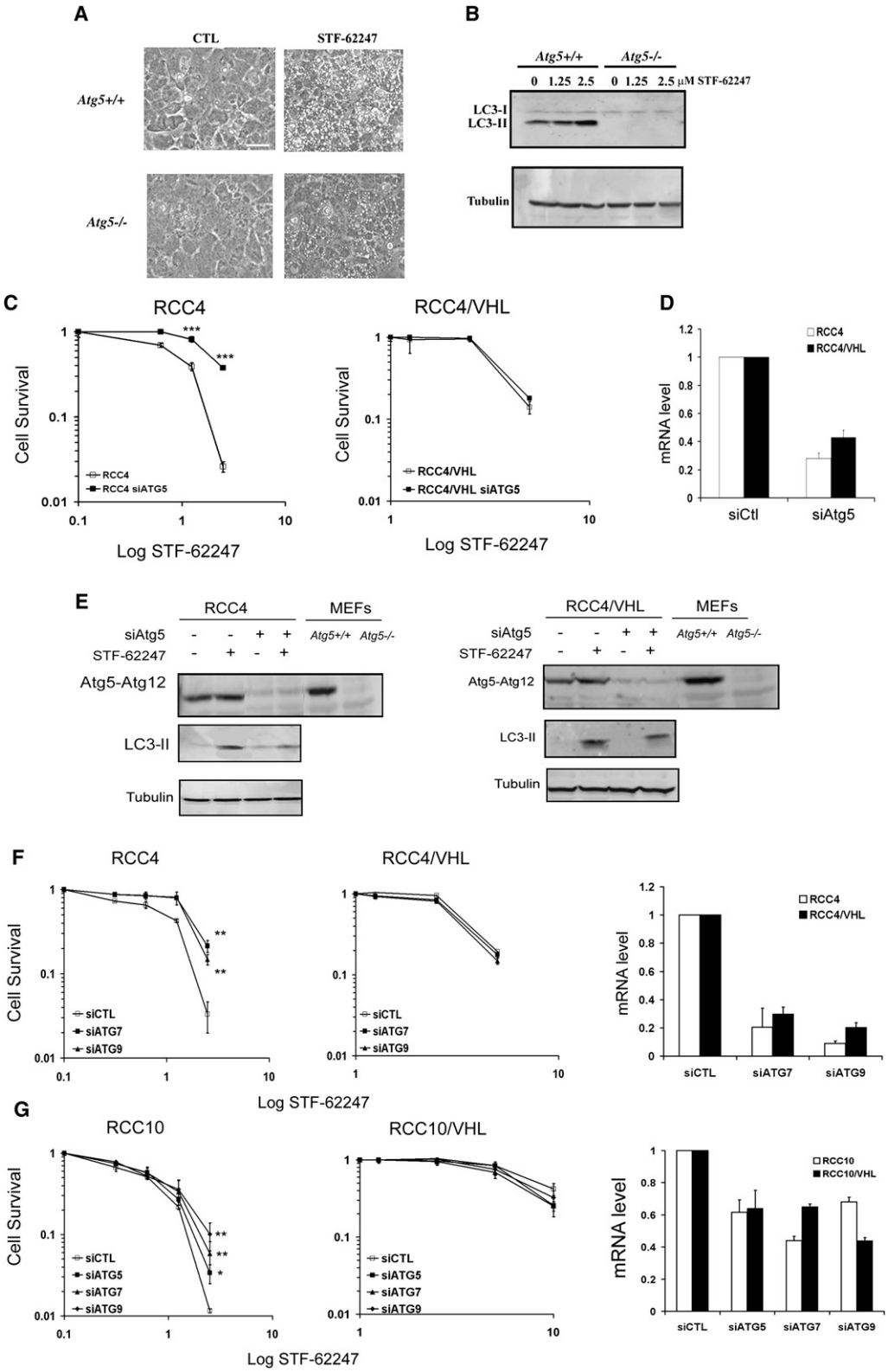

Figure 3. *ATG5* Is Involved in STF-62247 Autophagic Cell Death

(A) *Atg5*$^{+/+}$ and *Atg5*$^{-/-}$ murine embryonic fibroblasts (MEFs) were treated in presence of STF-62247 and examined under light microscopy 20 hr later. Scale bar = 10 μm.

(B) LC3 processing evaluated by western blot following 24 hr of drug treatment in MEFs.

reduced cell death induced by STF-62247 as assessed by clonogenic assay (Figure 3C). VHL-positive RCC4 cells were unaffected by *ATG5* siRNA, suggesting that the cell death observed at higher concentrations in VHL-positive cells is independent of *ATG5* and autophagy. A reduction in *ATG5-ATG12* levels by siRNA decreased LC3 formation by STF-62247, indicating a critical role for *ATG5* in the STF-62247 autophagic response in VHL-deficient RCC cells (Figure 3D). Consistent with a role of the autophagy pathway in STF-62247 cytotoxicity, reduction of *ATG7* and *ATG9* levels by siRNA also reduced the STF-62247 cytotoxicity in VHL-deficient RCC4 cells, although to a lesser degree (Figure 3F). Similar results were obtained using VHL-deficient RCC10 and RCC10 cells expressing wild-type VHL (Figure 3G).

PI3K and Golgi Trafficking Are Required as Initial Signals in STF-62247-Induced Autophagy

Previous studies have implicated PI3K and extracellular signal-regulated kinase (ERK) signaling as well as Golgi trafficking and endoplasmic reticulum (ER) stress in autophagy (Ogata et al., 2006; Yorimitsu et al., 2006). To evaluate a role for PI3K in response to STF-62247, we compared the effects of the autophagy inhibitor 3-MA to LY294002, another PI3K inhibitor. LY294002 significantly decreased large vacuole formation and the LC3-lipidated form in VHL-deficient cells during STF-62247 treatment to a level similar to 3-MA (Figures 4A and 4B; Figure 2D), indicating a role for PI3K in STF-62247 signaling. In contrast, the mitogen-activated protein kinase kinase (MEK) inhibitor U0126, which inhibits ERK activation, had little effect on autophagy induced by STF-62247 (Figures S3A and S3B), indicating that MEK signaling is not involved in STF-62247-induced autophagy.

Furthermore, we found that brefeldin A (BFA), a blocker of protein transport from the ER to the Golgi apparatus, abolished the formation of autophagic vacuoles and LC3-II stimulated by STF-62247 in VHL-deficient RCC cells. This suggests that Golgi trafficking is involved in the cytotoxicity of STF-62247 in cells that have lost VHL (Figures 4A–4C). In contrast, no vacuole or LC3 processing was observed with tunicamycin treatment alone, although it induced BiP (Grp78), a marker of ER stress (Figures S3A and S3C). Taken together, our results suggest that Golgi trafficking and PI3K are part of the initial signal for the induction of autophagy in RCC cells treated with STF-62247.

STF-62247 Increases Acidification in VHL-Deficient Cells

Although autophagosome formation in response to STF-62247 is independent of VHL status, we investigated how STF-62247 specifically kills cells that have lost VHL. A late step in the autophagic cell death process is the fusion of lysosomes with autophagosomes into autolysosomes, which can be detected by measuring their acidification with acridine orange staining. Interestingly, we found that acridine orange staining was significantly increased in VHL-deficient RCC4 cells compared to their wild-type VHL counterparts (Figure 4D). This observation was quantified and confirmed by fluorescence-activated cell sorting (FACS) analyses and illustrates a significant difference in the acidification of the acidic vesicular organelles (AVOs) in RCC4 and SN12C-VHL shRNA cells (Figures 4E and 4F; Figures S3D and S3E) compared to wild-type VHL cells. Blocking autophagy with 3-MA or BFA resulted in a decrease in autolysosomal acidification, demonstrating that acidification induced by STF-62247 is linked to the autophagic pathway. In addition, MDC staining performed using NH_4Cl to block vesicle acidification attenuated the functional staining following drug treatment (Figure S3F). However, even if the acidification level in VHL cells increases following STF-62247 treatment, this level of acidification remained significantly lower than in VHL-deficient cells. These results suggest that the fusion of autophagosomes with lysosomes is a key step leading to autophagic cell death in VHL-deficient cells.

Structure-Activity Studies

Based on the STF-62247 structure, other compounds were designed and synthesized to evaluate their ability to induce selective cell death in VHL-deficient cells. Analysis of the high-throughput screening data indicated a specific requirement for a 4-pyridyl unit linked to the 4-position of the thiazole, whereas 3-pyridyl analogs were inactive. The requirement of a thiazole NH suggests an H bond contact in this region. Substituents at the 2-position on the aryl ring were not tolerated. With these constraints in mind, we prepared a focused set of 19 analogs of STF-62247 to probe structure-activity relationships (Table S1). The IC_{50} for these analogs shows that STF-62247 has the lowest IC_{50} in VHL-deficient RCC4 cells and the highest IC_{50} ratio (VHL/VHL-deficient cells). The compound 30603 with a methyl group in the 4-position also has a high ratio, but also a higher IC_{50} for both RCC4 and RCC4/VHL cells. The IC_{50} could not be determined for some compounds because of poor solubility.

To associate the cytotoxicity of these compounds with autophagy, vacuole formation and LC3 processing were evaluated (Figures 5A and 5B). Compounds with an IC_{50} ratio VHL/VHL-deficient cells > 5 correlated positively with the presence of large vacuoles in VHL-deficient cells and the processing of LC3. As observed with STF-62247 treatment, the LC3-lipidated form was present in both wild-type VHL and VHL-deficient cell lines. To confirm that the cell death observed in VHL-deficient cells was associated with the acidification of autophagic vesicles, the level of AVOs was measured in response to five analogs (Figure 5C). The amount of AVOs was consistently higher in VHL-deficient cells treated with compounds 30603, 31184, and

(C) Cell survival measured by clonogenic assay with STF-62247 in RCC4 and RCC4/VHL cells transiently transfected with siRNA against *ATG5*. Colony formation was evaluated as described in Figure 1B. ***$p < 0.005$ between RCC4 and RCC4 with siATG5 in the presence of STF-62247.
(D) mRNA levels of *ATG5* quantified by qRT-PCR in RCC4 and RCC4/VHL cells transfected with siRNA against *ATG5* for 48 hr.
(E) Western blot for LC3 and ATG5 in RCC4 and RCC4/VHL cells transiently transfected with siRNA against *ATG5*. Tubulin was used as loading control.
(F and G) Left and middle panels: clonogenic assay with STF-62247 in cells transfected with *ATG7* and *ATG9* siRNA in VHL-deficient RCC4 (F) and RCC10 (G) cells and wild-type VHL cells. Colony formation was evaluated as described in Figure 1B. **$p < 0.01$ between siControl (siCTL) cells and siATG cells in response to STF-62247. Right panels: mRNA levels of *ATG7* and *ATG9* (and *ATG5* in RCC10 cells) quantified by qRT-PCR after 48 hr of transfection using siRNA against *ATG7* and *ATG9* (and *ATG5* in RCC10 cells) in RCC4 (F) and RCC10 (G) cells with or without VHL.
All error bars represent SEM.

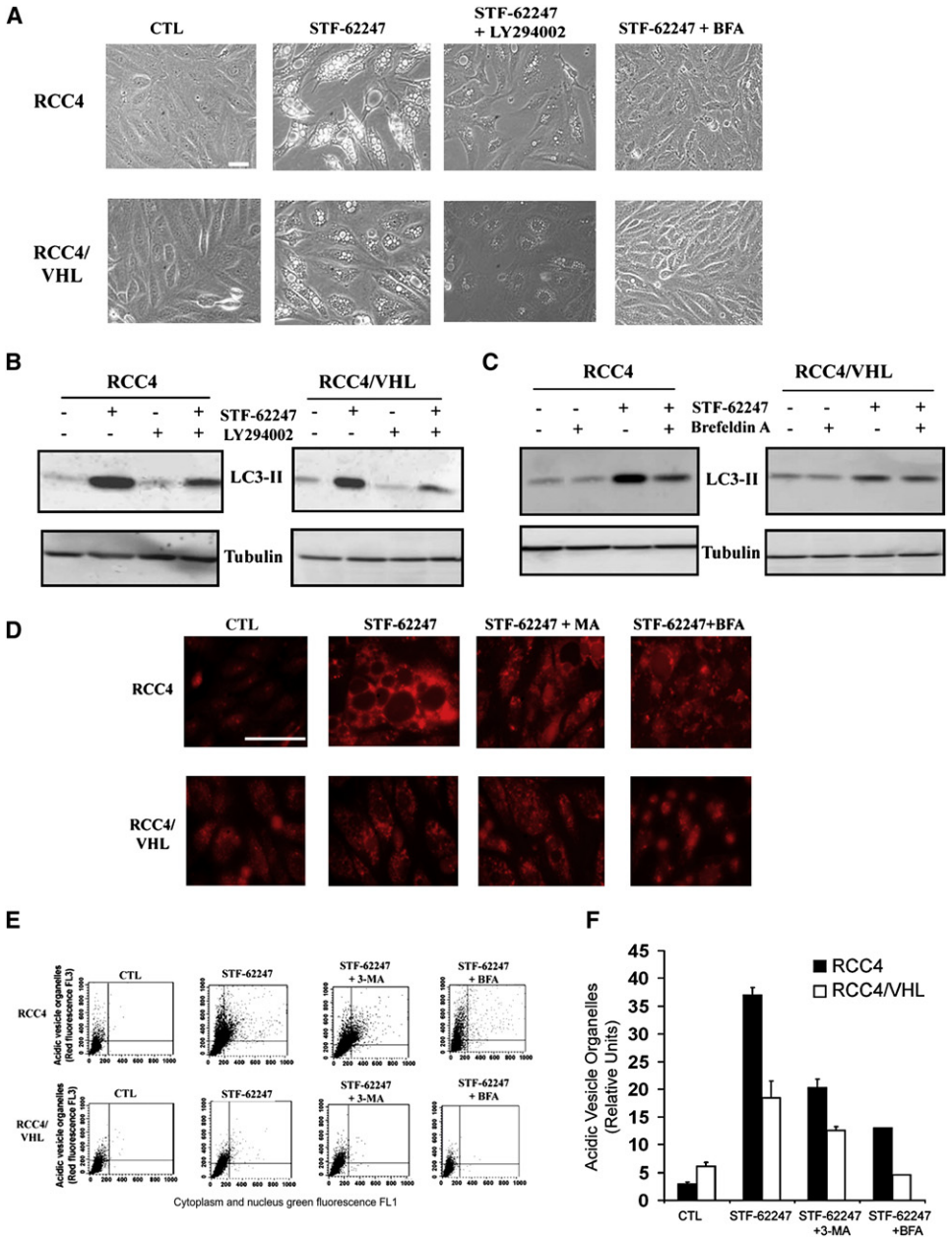

Figure 4. Golgi Trafficking and PI3K Are Involved in the STF-62247 Signaling Pathway and Acidification of Vesicles after STF-62247 Treatment

(A) VHL-deficient RCC4 and wild-type VHL cells were incubated in presence of 10 μM LY294002 or 1 μg/ml brefeldin A (BFA) with 1.25 μM STF-62247 for 20 hr, and the presence of vacuoles was examined by light microscopy.

(B and C) LC3 processing was evaluated by western blot after treatment with brefeldin A or LY294002 in the presence or absence of STF-62247. Tubulin was used as loading control.

(D) Cells were treated with 1.25 μM STF-62247 with or without 2 mM 3-MA or 1 μg/ml brefeldin A for 20 hr. For the last 15 min, acidic components were stained with 1 μg/ml acridine orange and visualized by fluorescence microscopy.

(E) Fluorescence-activated cell sorting (FACS) analysis measuring acidic vesicular organelles (AVOs) in cells treated in (D). The y axis represents the concentrated red dye in the acidic vesicles, whereas the x axis represents green fluorescence in the cytoplasm and nucleus.

(F) Quantification of the FACS analysis. The data are calculated as the average of three different experiments as relative units of treated over untreated cells. All error bars represent SEM. All scale bars = 10 μm.

30651, which had relatively low IC_{50} and induced significant vacuole formation and the LC3-lipidated form. In contrast, AVO staining was not influenced in response to compound 31185 and 31270, which induced neither autophagy nor cytotoxicity. These results confirm that the autophagic cell death observed in VHL-deficient cells is dependent on the acidification of the

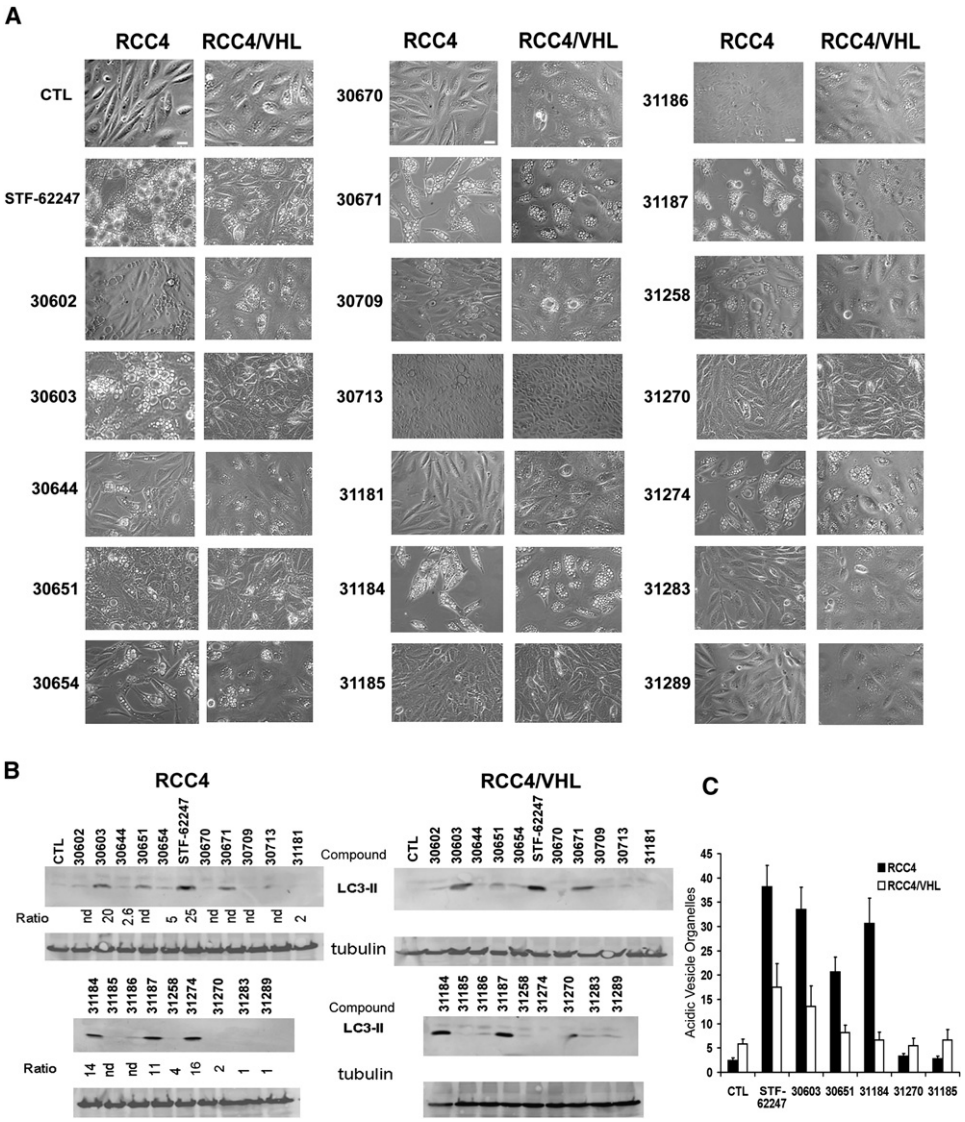

Figure 5. Evaluation of Autophagy in Renal Cell Carcinomas Treated with Analogs of STF-62247

(A) RCC4 and RCC4/VHL cells were treated with a 1.25 μM concentration of each of 19 analogs for 20 hr, and the presence of vacuoles was examined by light microscopy. Scale bars = 10 μm.

(B) Western blot for LC3 after treatment with each compound. Tubulin was used as loading control. "Ratio" is the IC_{50} in RCC4/VHL cells relative to the IC_{50} in RCC4 cells.

(C) AVOs measured by FACS analysis in cells treated with 1.25 μM STF-62247 or with compounds 30603, 30651, 31184, 31270, and 31185 and stained with acridine orange. Error bars represent SEM.

vacuoles. The strong relationship between autophagic cell death and vacuole acidification might explain why autophagy leads to cell death in VHL-deficient cells and not in wild-type cells.

Use of a Yeast Deletion Pool to Identify Targets of STF-62247

To identify a target for STF-62247, we performed a screen of a yeast deletion pool to determine which genes affect STF-62247 sensitivity. We found that cells lacking proteins involved in Golgi trafficking and in morphogenesis were most sensitive to STF-62247 (Table S2). To validate the data obtained from this screen, we evaluated the sensitivity of eight yeast deletion strains following STF-62247 treatment (Figure 6A). The killing curves for the *CLA4*, *VPS20*, *ALG5*, *OSH3*, and *YPT31* deletion strains show significant toxicity in response to STF-62247. The *ATG8* deletion strain did not exhibit sensitivity to STF-62247 as expected based on our human ATG studies (data not shown). The human orthologs known for *CLA4*, *VPS20*, *ALG5*, *OSH3*, and *YPT31* are *PAK2*, *CHMP6*, *ALG5*, *OSBPL3*, and *RAB11A*, respectively. In mammalian cells, we found that the expression of *ALG5*, *OSBPL3*, and *CHMP6* correlated with VHL status (Figure 6B). These three proteins play a role in coordinating vesicular transport between the ER, the TGN, and lysosomes. Moreover, the knockdown of these proteins using siRNA

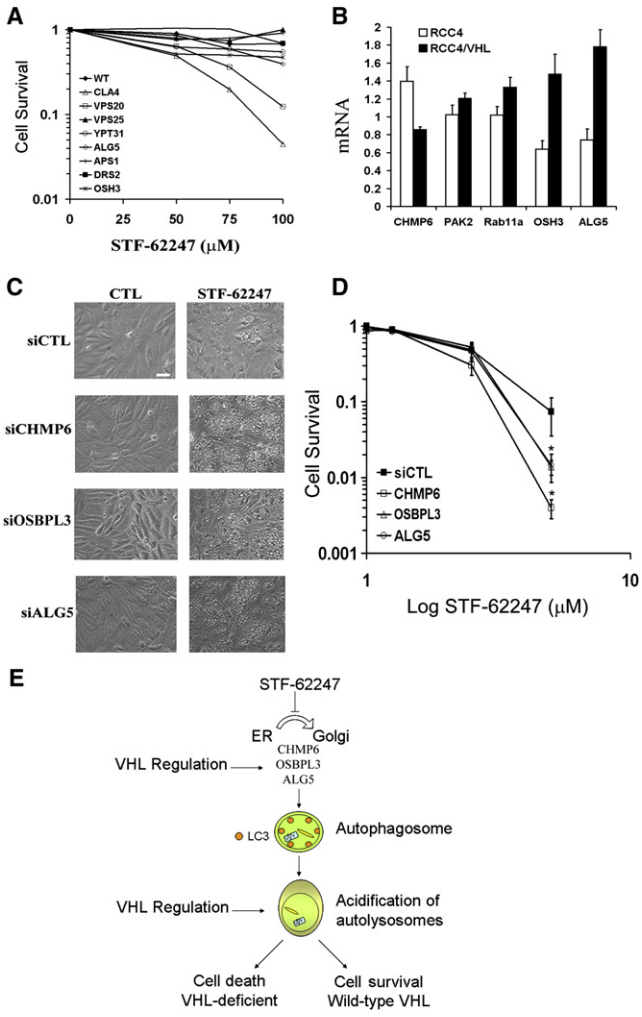

Figure 6. Golgi Trafficking Proteins Are Sensitive and Are a Target for STF-62247

(A) Killing curves for eight yeast deletion strains. Wild-type (WT), *CLA4*, *VPS20*, *VPS25*, *YPT31*, *ALG5*, *APS1*, *DRS2*, and *OSH3* were incubated with STF-62247 (0–100 μM) for 1 hr, and colony formation was evaluated after 2 days. Each point of survival is calculated by the average of two different experiments in triplicate as the percent of treated on untreated plate.

(B) qRT-PCR for *CHMP6*, *PAK2*, *RAB11a*, *OSBPL3*, and *ALG5* in RCC4 and RCC4/VHL cells. The histogram is calculated by the average of three different experiments in triplicate as the percent of RCC4/VHL on RCC4 cells. Error bars represent SEM.

(C) VHL cells were transiently transfected with siRNA for *CHMP6*, *OSBPL3*, and *ALG5* for 72 hr. For the last 24 hr, 1.25 μM STF-62247 was added, and vacuole formation was examined by light microscopy. Scale bar = 10 μm.

(D) Clonogenic assay with STF-62247 (0–30 μM) in RCC4/VHL cells transiently transfected in the same conditions as in (C). Colony formation was evaluated as described in Figure 1B. Error bars represent SEM. *$p < 0.05$ between VHL cells and VHL cells with siRNA in presence of 5 μM STF-62247.

(E) Representative schema of the effect of STF-62247 in renal cell carcinomas through autophagy. STF-62247 disrupts ER-Golgi trafficking through CHMP6, OSBPL3, and ALG5 and induces autophagy. Lipidation of LC3 associated with the double membrane of the autophagosome is observed in an *ATG5*-dependent manner. Higher acidification of autolysosomes is associated with autophagic cell death in VHL-deficient cells, whereas wild-type VHL cells are protected against acidification and survive. Regulation of CHMP6, OSBPL3, and ALG5 proteins by VHL is also observed and remains to be investigated.

(Figure S4) increased vacuole formation in response to STF-62247 (Figure 6C) and cytotoxicity in VHL cells, suggesting that their loss partially phenocopies the loss of VHL (Figure 6D). Taken together, our results demonstrate that the TGN is a target of STF-62247 and a drug-selective pathway synthetically lethal in VHL-deficient cells.

DISCUSSION

Targeting HIF in cancer therapy is being investigated ardently. Different screening approaches have identified drugs, cytotoxins or small molecules, as HIF inhibitors. It has been reported that radiation in combination with a HIF inhibitor could improve conventional therapies (Moeller et al., 2005). In RCCs with constitutively elevated levels of HIF, different agents that can disrupt or attenuate the HIF pathway or the protein products of HIF target genes are presently in clinical trials or have been approved by the US Food and Drug Administration (FDA). For example, temsirolimus (CCI-779) and everolimus (RAD001) inhibit HIF through the targeting of mTOR. In contrast, agents with antiangiogenic activity that inhibit vascular endothelial growth factor receptor (VEGFR) and platelet-derived growth factor receptor (PDGFR) signaling (e.g., sorafenib and sunitinib), the VEGF ligand (bevacizumab), and the epidermal growth factor (EGF) ligand (cetuximab) have also shown some effectiveness in the management of RCC to different degrees (Patel et al., 2006; Sosman et al., 2007). These agents have all been reported to have antitumor effects on kidney tumors, but tumors ultimately progress regardless of these therapies, as they are not cytotoxic but cytostatic. In the kidney, the inactivation of the tumor suppressor gene *VHL* is an early event that promotes tumorigenesis, leading to clear cell RCC. We hypothesized that inactivation of VHL in RCC progression could be therapeutically exploited using a screening strategy that targets cells with loss of VHL. While different agents have been used to target the HIF pathway, we investigated an approach of using small molecules to induce selective cell death in RCCs that lack a functional *VHL* gene, the mammalian equivalent of a yeast synthetic lethal screen. Among the drugs identified from this screen (unpublished data), we found that STF-62247 was cytotoxic to VHL-deficient cells. Surprisingly, cell death induced by STF-62247 was independent of HIF-1α or HIF-2α and was unaffected by hypoxia (data not shown). Our results support other reports demonstrating that in addition to its well-understood role in HIF degradation, VHL has other critical targets that also play important roles in cellular homeostasis (Hergovich et al., 2003; Lolkema et al., 2005; Na et al., 2003; Ohh et al., 1998; Okuda et al., 2001).

It has been proposed that the resistance of RCCs to chemotherapy and radiotherapy is due to increased levels of nuclear factor κB (NF-κB) activity and resistance to apoptosis (An et al., 2005; Oya et al., 2001; Qi and Ohh, 2003). Previous studies have reported that the metabolic stress observed in human tumors leads cancer cells to acquire resistance to apoptosis and to stimulate autophagy to maintain energy demand and prevent necrosis (Jin et al., 2007). Increasing evidence implicates a role for autophagy in cancer, but it is still not well understood how cellular and environmental cues drive autophagic cells down survival or death pathways (Jin et al., 2007; Mathew et al., 2007). It has been reported that above a certain threshold that destroys

organelles and portions of the cytoplasm, autophagic cell death is induced (Gozuacik and Kimchi, 2007). It is also possible that autophagy can kill by selective degradation of vital proteins in the cell. Anticancer therapies using radiation or agents such as tamoxifen, rapamycin, imatinib, arsenic trioxide, resveratrol, or soybean B group saponins have recently been reported to induce autophagic cell death (Bursch et al., 1996; Ellington et al., 2005; Ertmer et al., 2007; Ito et al., 2005; Kanzawa et al., 2003; Opipari et al., 2004; Takeuchi et al., 2005). We provide evidence that STF-62247 induces autophagy and that inhibition of autophagy significantly increases the survival of VHL-deficient cells treated with STF-62247.

Among different stimuli, signaling cascades, and proteins that have been reported to be involved in the initial signal for autophagy, ER stress and Golgi trafficking have been identified in the formation of autophagosomes (Ogata et al., 2006; Yorimitsu et al., 2006; Young et al., 2006). The PI3K-beclin 1 (*ATG6*) complex (Furuya et al., 2005), the PI3K/AKT/mTOR cascade (Takeuchi et al., 2005), the Ras/MEK/ERK pathway (Corcelle et al., 2006), and the p53/p73 family (Crighton et al., 2006, 2007) have also been found to regulate the autophagic process. Thus, it appears that the upstream signals that induce autophagy are stimulus and organism dependent. In our study, we show that the Golgi trafficking and PI3K pathways are involved in the STF-62247 upstream signal for autophagosome formation. More specifically, yeast deletion strains for *ALG5*, *OSH3*, and *VPS20* are sensitive to STF-62247. In mammalian cells, knockdown of the equivalent protein orthologs (ALG5, OSBPL3, and CHMP6, respectively) that are located in the ER and the TGN was found to be lethal in combination with STF-62247 in cells with functional VHL. While knockdown of ALG5, an enzyme found in the membrane of the ER, sensitizes the cell to death in cells with functional VHL, ER stress induced by tunicamycin had no apparent effect in response to STF-62247. ALG5 catalyzes the transfer of glucose from UDP-glucose to dolichyl phosphate. A deletion of the yeast *ALG5* gene leads to a loss of this activity and an underglycosylation of carboxypeptidase Y (Heesen et al., 1994). However, the ER stress induced by tunicamycin that leads to autophagy increases the unfolded protein response (UPR) and induces the expression of chaperones and proteins involved in the recovery process (Yorimitsu et al., 2006). ER stress-induced autophagy has been reported in yeast and in neuroblastoma but is distinct from autophagy induced by STF-62247 (Ogata et al., 2006; Yorimitsu et al., 2006). Our results also show that oxysterol-binding protein-like protein 3 (OSBPL3), a protein involved in a variety of processes such as secretory vesicle budding from the Golgi and establishment of cell polarity; the glucosyltransferase ALG5; and CHMP6, a key component of the endosomal sorting complex required for transport-III (ESCRT-III) required for protein transport into the multivesicular body pathway to the lysosomal/vacuolar lumen, are regulated by VHL (Castro et al., 1999; Perry and Ridgway, 2006; Yorikawa et al., 2005). However, the mechanism of regulation of these proteins by VHL is unknown and remains to be investigated. Recently, it was reported that disruption of the ESCRT-III complex induces autophagosome formation and neurodegeneration consistent with our results (Lee et al., 2007). A role for sterol proteins in elongation of the autophagosome membrane has previously been demonstrated (Nazarko et al., 2007). In addition, STF-62247-induced autophagy was blocked in the presence of BFA, a compound that causes the TGN to reassemble into extensive tubular processes and merge with the recycling endosomal system. Our results suggest that certain proteins associated with the TGN and the ER are targeted by STF-62247 in VHL-deficient RCCs. Furthermore, we show that ATG9, the only transmembrane ATG, is involved in autophagic cell death in response to STF-62247. Mammalian *ATG9* has been implicated in trafficking between the Golgi and endosomes, supporting a role for the Golgi in the initial signal of autophagy (Young et al., 2006). Recently, a study reported that the transcript of sONE, an antisense of eNOS and a yeast homolog of ATG9, is upregulated in the absence of VHL function in a HIF-independent mechanism and may interfere with the HuR/VHL interaction (Fish et al., 2007).

We established that autophagosome formation occurs in both VHL-deficient and wild-type VHL cells after STF-62247 treatment. Interestingly, our analyses indicate that the drug stimulates the maturation of autophagosomes into autolysosomes in VHL-deficient cells and that the size of autolysosomes is larger in VHL-deficient cells. The acidification present after fusion with the lysosomes in VHL-inactivated cells was prevented by treatment with NH_4Cl (Figure S3F). Although the fusion of autophagosomes with lysosomes is known, the maturation steps and proteins implicated remain to be elucidated. It has been reported that microtubules (Kochl et al., 2006), the GTPase Rab7 (Gutierrez et al., 2004), and the lysosome-associated membrane proteins 1 and 2 (LAMP1 and 2) (Eskelinen et al., 2002) are essential for the endosome/lysosome fusion process. Disruption or inactivation of these proteins has been shown to block the maturation of autophagic vacuoles, likely before the fusion with the lysosomes. Preliminary results indicate that knockdown of LAMP1 or LAMP2 does not influence the toxicity of STF-62247 in VHL-deficient cells or in cells with functional VHL and therefore cannot explain the difference in acidic vesicular organelles observed. However, our results suggest that VHL-deficient cells are altered in the autolysosomal maturation step, increasing the acidification of vesicular organelles.

Many chemotherapeutic agents are limited in their therapeutic index due to their cytotoxicity to nontumor cells. To develop new compounds with higher therapeutic indices, targeted genetic approaches should be considered (Giaccia et al., 2003; Sutphin et al., 2004). Synthetic lethality describes a combination of two nonallelic mutations that, although individually nonlethal, together result in cell death. This concept has been used successfully in yeast and *Drosophila* and shows a potential means of achieving selective toxicity based on genotypic differences between tumor cells and normal tissue (Hartman et al., 2001; Kaelin, 2005). In this study, we found that renal cancer cells deficient in VHL were sensitive to the small molecule STF-62247, whereas cells with wild-type VHL were unaffected by STF-62247 treatment, establishing a synthetic lethal situation wherein both drug treatment and VHL deficiency lead to lethality. We also identified proteins involved in Golgi trafficking as a targeting pathway for STF-62247 and demonstrated that STF-62247 in combination with the loss of VHL leads to synthetic lethality. This synthetic lethal approach should be considered in the future for the continued development of other molecular targeting

agents for the treatment of RCC, as they have the benefit of selectively killing tumor cells based on their genotype.

EXPERIMENTAL PROCEDURES

Cell Culture and Cell Treatments

RCC4 parental cells and RCC4 cells with VHL reintroduced (RCC4/VHL), SN12C and SN12C-CSCG-VHL shRNA (gift from George V. Thomas, University of California, Los Angeles), and *Atg5*$^{+/+}$ and *Atg5*$^{-/-}$ murine embryonic fibroblasts (MEFs) (gift from Noboru Mizushima, Tokyo Medical and Dental University) were maintained in DMEM supplemented with 10% FCS. Cells were plated at 70% confluency and treated with 1.25 μM (RCC4) or 3.75 μM (SN12C) STF-62247 overnight in presence or absence of 2 mM 3-MA, 1 μg/ml brefeldin A, 10 μM LY294002, 2 μg/ml tunicamycin, or 10 μM U0126 (Sigma Chemical Co.).

Cell Viability Assays

For cell viability assays, 100,000 cells were plated in a 12-well plate. The following day, 1.25 μM STF-62247 was added in the presence or absence of 1 mM 3-MA for 24 hr at 37°C. Cells were trypsinized and counted by trypan blue exclusion. For 2,3-bis[2-methoxy-4-nitro-5-sulfophenyl]-2H-tetrazolium-5-carboxanilide (XTT) assays, 5,000 RCC4 cells with and without VHL or 2,500 SN12C cells with and without VHL shRNA were plated in 96-well plates. The following day, vehicle (DMSO), STF-62247, or each of 19 analogs were added to media by serial dilution. Four days later, the media were aspirated, and XTT solution containing 0.3 mg/ml of XTT (Sigma Chemical Co.) in phenol red-free media, 20% FCS, and 2.65 mg/ml N-methyl dibenzopyrazine methyl sulfate (PMS) was added to the cells and incubated at 37°C for 1–2 hr. Metabolism of XTT was quantified by measuring the absorbance at 450 nm on a plate reader.

Clonogenic Cell Survival Assay

RCC4, RCC4/VHL, SN12C, and SN12C-VHL shRNA cells were plated at 300 cells per 60 mm tissue culture dish. The following day, vehicle or STF-62247 was added, and cells were incubated in the presence of drug for 10 days for RCC4 and RCC4/VHL and 7–10 days for SN12C and SN12C-VHL shRNA. The colonies were stained with crystal violet and quantified. Each experiment was performed at least three times in triplicate.

Western Blot Analysis

After treatments, cells were lysed in urea buffer (9 M urea, 75 mM Tris [pH 7.5], 150 mM β-mercaptoethanol), placed on ice for 10 min, and sonicated briefly (15 s). Extracts were centrifuged at 8000 × g for 10 min to eliminate insoluble material. Lysates were quantitated using Bio-Rad Protein Assay, and 20–30 μg quantities of proteins were separated on 7.5% or 15% bis-acrylamide gels and then transferred onto PVDF membranes. Proteins were visualized using HIF-2α (Novus Biological), HIF-1α, pVHL, and BiP (BD Biosciences), LC3 (MBL), Atg5 (gift from N. Mizushima), or α-tubulin antibodies.

Quantification of Acidic Vesicle Organelles with Acridine Orange

In acridine orange-stained cells, the cytoplasm and nucleus are bright green and dim red whereas acidic compartments are bright red. The intensity of the red fluorescence is proportional to the degree of acidity. Following 20 hr of treatment with STF-62247 or analogs, cells were stained with 1 μg/ml of acridine orange for 15 min. Cells were trypsinized and then analyzed by flow cytometry using a FACScan cytometer (BD Biosciences) and CellQuest software.

Immunofluorescence Staining

Cells were seeded on glass coverslips, and STF-62247 was added at subconfluence at 1.25 μM for RCC4 and 3.75 μM for SN12C. After 20 hr, cells were fixed in 3.7% formaldehyde for 10 min at room temperature and washed in PBS. Cells were then permeabilized in 0.2% Triton X-100 for 5 min at room temperature and washed in PBS. The coverslips were incubated with primary LC3 antibody diluted 1:500 in PBS containing 0.2% BSA for 1 hr at room temperature. Cells were washed three times in PBS-BSA, and the bound primary antibody was detected using a fluorescein-conjugated secondary antibody (Alexa 488) diluted 1:500 in PBS-BSA and incubated for 1 hr. Coverslips were washed and mounted in mounting medium (Vector Laboratories) according to the manufacturer's instructions. Cells were examined with a confocal microscope.

Visualization of MDC Vacuoles

Cell were incubated in the presence of drug for 20 hr and labeled with a 50 mM concentration of the autofluorescent marker monodansylcadaverine (MDC) (Sigma Chemical Co.) in PBS at 37°C for 10 min. Cells were then fixed with 3.7% formaldehyde for 10 min at room temperature and washed in PBS. MDC was observed by fluorescence microscopy with a Nikon Eclipse E800.

In Vivo Studies

All animal experiments were performed in accordance with institutional and national guidelines and approved by Stanford University's Administrative Panel on Laboratory Animal Care (APLAC). Male SCID mice, 4 to 6 weeks old, were obtained from either Stanford University's Research Animal Facility or Charles River Laboratories. SN12C (2–3 × 10^6), SN12C-VHL shRNA (2–3 × 10^6), or 786-O (5 × 10^6) cells were resuspended in sterile PBS and injected subcutaneously. Mice were randomized into vehicle control group or treatment group and treated daily by intraperitoneal injection. When tumors reached 100 mm^3, mice in the treatment group implanted with SN12C or SN12C-VHL shRNA cells were treated with 8 mg/kg or 2.7 mg/kg of STF-62247, whereas 2 weeks after 786-O cell implantation, mice were treated with 8 mg/kg of STF-62247. Tumor growth was measured every 2–3 days after drug treatment was started.

shRNA Constructs, Plasmids, and Retroviral Infection

The CMV-EYFP fluorescent protein and the HIF-2α P531A N847A double mutant were cloned into pBabe-puro vector. The sequences used for HIF-1α and HIF-2α shRNA were GAGGAACTACCATTATAT and GGAGACG GAGGTGGTCTAT, respectively. Retroviruses were produced by transfecting plasmids into ΦNX amphotropic cell lines according to the manufacturer's instructions with Lipofectamine Plus (Invitrogen). The next day after transfection, cells were placed at 32°C. Retroviruses were harvested 48 and 72 hr after transfection. Puromycin was used to select for stable retroviral integrants.

Transient Transfection of RCCs

Cells were transfected with siRNA against *ATG5*, *CHMP6*, *PAK2*, *RAB11a*, *OSBPL3*, *ALG5*, *ATG7*, *ATG9* (SMARTpool), and siControl2 nontargeting pool from Dharmacon using Dharmafect reagent 1 for 48 hr. Cells were split for clonogenic assay and harvested for RNA or protein.

Screen in Yeast and Killing Curves

Genotypes of the parental yeast strain BY4743, construction of the homozygous diploid deletion strains, and construction of the homozygous diploid deletion pool were as described previously (Thomas et al., 2006). A mutant pool of 4728 nonessential homozygous diploid deletion strains was used. The parental diploid strain BY4743 was used as a control in survival and complementation assays. For clonogenic survival, equivalent numbers of early log-phase parental and deletion strains for *ALG5*, *APS1*, *OSH3*, *CLA4*, *DRS2*, *DAP1*, *VPS20*, *VPS25*, *FIG4*, and *SPT4* were suspended in yeast extract peptone dextrose (YPD) and treated with STF-62247 (0–100 μM) for 1 hr while being shaken at 300 rpm at 30°C. Cells were then pelleted, washed once with buffer (10 mM Tris, 5 mM EDTA), pelleted, and resuspended in the same buffer. Cells were then plated at appropriate dilutions onto YPD solid medium to allow for accurate counting of surviving colonies (range 50–250). Plates were incubated for 2 days at 30°C before counting colonies. Full survival curves were performed in triplicate for each selected deletion strain.

Quantitative RT-PCR

RNA from cells transfected with siControl or siAtg was prepared using TRIzol (Invitrogen) according to the manufacturer's protocol. Reverse transcription (RT) was performed with Moloney murine leukemia virus (MMLV) reverse transcriptase (Invitrogen) using 2 μg of RNA and 5 μM random primers (Invitrogen) according to the manufacturer's instructions. Approximately 0.5% of each RT reaction was used for quantitative RT-PCR reactions containing 5 μl 2× SYBR green master mix (ABI) and 200 nM forward and reverse primers specific to the different genes of interest in a volume of 10 μl. Detection and data analysis were carried out with an ABI PRISM 7900 sequence detection system using

TBP primers as an internal control. PCR primer sequences were obtained from the Primer Bank database (http://pga.mgh.harvard.edu/primerbank/), and primers were synthesized in the Stanford Protein and Nucleic Acid Biotechnology Facility.

SUPPLEMENTAL DATA

The Supplemental Data include two tables, four figures, and two movies and can be found with this article online at http://www.cancercell.org/cgi/content/full/14/1/90/DC1/.

ACKNOWLEDGMENTS

This work was supported by a gift from the Silicon Valley Community Foundation (A.J.G.), a Canadian Institutes of Health Research Fellowship (S.T.), and NCI/NIH grants NCI-CA-082566 (A.J.G.) and NCI-CA-123823 (D.A.C.). The authors would like to thank N. Mizushima for *Atg5* MEFs and Atg5 antibody and G.V. Thomas for SN12C and SN12C-VHL shRNA cells. The authors would also like to thank Martin Brown, James Brown, and Kelly McCann for their technical assistance with the yeast deletion pool and Trent A. Watkins for help with the time-lapse microscopy.

Received: October 17, 2007
Revised: February 2, 2008
Accepted: June 9, 2008
Published: July 7, 2008

REFERENCES

Aita, V.M., Liang, X.H., Murty, V.V., Pincus, D.L., Yu, W., Cayanis, E., Kalachikov, S., Gilliam, T.C., and Levine, B. (1999). Cloning and genomic organization of beclin 1, a candidate tumor suppressor gene on chromosome 17q21. Genomics *59*, 59–65.

An, J., Fisher, M., and Rettig, M.B. (2005). VHL expression in renal cell carcinoma sensitizes to bortezomib (PS-341) through an NF-kappaB-dependent mechanism. Oncogene *24*, 1563–1570.

Bursch, W., Ellinger, A., Kienzl, H., Torok, L., Pandey, S., Sikorska, M., Walker, R., and Hermann, R.S. (1996). Active cell death induced by the anti-estrogens tamoxifen and ICI 164 384 in human mammary carcinoma cells (MCF-7) in culture: the role of autophagy. Carcinogenesis *17*, 1595–1607.

Castro, O., Chen, L.Y., Parodi, A.J., and Abeijon, C. (1999). Uridine diphosphate-glucose transport into the endoplasmic reticulum of Saccharomyces cerevisiae: in vivo and in vitro evidence. Mol. Biol. Cell *10*, 1019–1030.

Chan, D.A., Sutphin, P.D., Denko, N.C., and Giaccia, A.J. (2002). Role of prolyl hydroxylation in oncogenically stabilized hypoxia-inducible factor-1alpha. J. Biol. Chem. *277*, 40112–40117.

Corcelle, E., Nebout, M., Bekri, S., Gauthier, N., Hofman, P., Poujeol, P., Fenichel, P., and Mograbi, B. (2006). Disruption of autophagy at the maturation step by the carcinogen lindane is associated with the sustained mitogen-activated protein kinase/extracellular signal-regulated kinase activity. Cancer Res. *66*, 6861–6870.

Crighton, D., Wilkinson, S., O'Prey, J., Syed, N., Smith, P., Harrison, P.R., Gasco, M., Garrone, O., Crook, T., and Ryan, K.M. (2006). DRAM, a p53-induced modulator of autophagy, is critical for apoptosis. Cell *126*, 121–134.

Crighton, D., O'Prey, J., Bell, H.S., and Ryan, K.M. (2007). p73 regulates DRAM-independent autophagy that does not contribute to programmed cell death. Cell Death Differ. *14*, 1071–1079.

Ellington, A.A., Berhow, M., and Singletary, K.W. (2005). Induction of macroautophagy in human colon cancer cells by soybean B-group triterpenoid saponins. Carcinogenesis *26*, 159–167.

Erler, J.T., Bennewith, K.L., Nicolau, M., Dornhofer, N., Kong, C., Le, Q.T., Chi, J.T., Jeffrey, S.S., and Giaccia, A.J. (2006). Lysyl oxidase is essential for hypoxia-induced metastasis. Nature *440*, 1222–1226.

Ertmer, A., Huber, V., Gilch, S., Yoshimori, T., Erfle, V., Duyster, J., Elsasser, H.P., and Schatzl, H.M. (2007). The anticancer drug imatinib induces cellular autophagy. Leukemia *21*, 936–942.

Eskelinen, E.L., Illert, A.L., Tanaka, Y., Schwarzmann, G., Blanz, J., Von Figura, K., and Saftig, P. (2002). Role of LAMP-2 in lysosome biogenesis and autophagy. Mol. Biol. Cell *13*, 3355–3368.

Fish, J.E., Matouk, C.C., Yeboah, E., Bevan, S.C., Khan, M., Patil, K., Ohh, M., and Marsden, P.A. (2007). Hypoxia-inducible expression of a natural cis-antisense transcript inhibits endothelial nitric-oxide synthase. J. Biol. Chem. *282*, 15652–15666.

Furuya, N., Yu, J., Byfield, M., Pattingre, S., and Levine, B. (2005). The evolutionarily conserved domain of Beclin 1 is required for Vps34 binding, autophagy and tumor suppressor function. Autophagy *1*, 46–52.

Giaccia, A., Siim, B.G., and Johnson, R.S. (2003). HIF-1 as a target for drug development. Nat. Rev. Drug Discov. *2*, 803–811.

Gnarra, J.R., Zhou, S., Merrill, M.J., Wagner, J.R., Krumm, A., Papavassiliou, E., Oldfield, E.H., Klausner, R.D., and Linehan, W.M. (1996). Post-transcriptional regulation of vascular endothelial growth factor mRNA by the product of the VHL tumor suppressor gene. Proc. Natl. Acad. Sci. USA *93*, 10589–10594.

Gozuacik, D., and Kimchi, A. (2007). Autophagy and cell death. Curr. Top. Dev. Biol. *78*, 217–245.

Gutierrez, M.G., Munafo, D.B., Beron, W., and Colombo, M.I. (2004). Rab7 is required for the normal progression of the autophagic pathway in mammalian cells. J. Cell Sci. *117*, 2687–2697.

Hartman, J.L., 4th, Garvik, B., and Hartwell, L. (2001). Principles for the buffering of genetic variation. Science *291*, 1001–1004.

Heesen, S., Lehle, L., Weissmann, A., and Aebi, M. (1994). Isolation of the ALG5 locus encoding the UDP-glucose:dolichyl-phosphate glucosyltransferase from Saccharomyces cerevisiae. Eur. J. Biochem. *224*, 71–79.

Hergovich, A., Lisztwan, J., Barry, R., Ballschmieter, P., and Krek, W. (2003). Regulation of microtubule stability by the von Hippel-Lindau tumour suppressor protein pVHL. Nat. Cell Biol. *5*, 64–70.

Iliopoulos, O., Kibel, A., Gray, S., and Kaelin, W.G., Jr. (1995). Tumour suppression by the human von Hippel-Lindau gene product. Nat. Med. *1*, 822–826.

Iliopoulos, O., Levy, A.P., Jiang, C., Kaelin, W.G., Jr., and Goldberg, M.A. (1996). Negative regulation of hypoxia-inducible genes by the von Hippel-Lindau protein. Proc. Natl. Acad. Sci. USA *93*, 10595–10599.

Isaacs, J.S., Jung, Y.J., Mimnaugh, E.G., Martinez, A., Cuttitta, F., and Neckers, L.M. (2002). Hsp90 regulates a von Hippel Lindau-independent hypoxia-inducible factor-1 alpha-degradative pathway. J. Biol. Chem. *277*, 29936–29944.

Ito, H., Daido, S., Kanzawa, T., Kondo, S., and Kondo, Y. (2005). Radiation-induced autophagy is associated with LC3 and its inhibition sensitizes malignant glioma cells. Int. J. Oncol. *26*, 1401–1410.

Ivan, M., Kondo, K., Yang, H., Kim, W., Valiando, J., Ohh, M., Salic, A., Asara, J.M., Lane, W.S., and Kaelin, W.G., Jr. (2001). HIFalpha targeted for VHL-mediated destruction by proline hydroxylation: implications for O2 sensing. Science *292*, 464–468.

Jaakkola, P., Mole, D.R., Tian, Y.M., Wilson, M.I., Gielbert, J., Gaskell, S.J., Kriegsheim, A., Hebestreit, H.F., Mukherji, M., Schofield, C.J., et al. (2001). Targeting of HIF-alpha to the von Hippel-Lindau ubiquitylation complex by O2-regulated prolyl hydroxylation. Science *292*, 468–472.

Jin, S., Dipaola, R.S., Mathew, R., and White, E. (2007). Metabolic catastrophe as a means to cancer cell death. J. Cell Sci. *120*, 379–383.

Kabeya, Y., Mizushima, N., Ueno, T., Yamamoto, A., Kirisako, T., Noda, T., Kominami, E., Ohsumi, Y., and Yoshimori, T. (2000). LC3, a mammalian homologue of yeast Apg8p, is localized in autophagosome membranes after processing. EMBO J. *19*, 5720–5728.

Kaelin, W.G., Jr. (2005). The concept of synthetic lethality in the context of anticancer therapy. Nat. Rev. Cancer *5*, 689–698.

Kanzawa, T., Kondo, Y., Ito, H., Kondo, S., and Germano, I. (2003). Induction of autophagic cell death in malignant glioma cells by arsenic trioxide. Cancer Res. *63*, 2103–2108.

Kihara, A., Kabeya, Y., Ohsumi, Y., and Yoshimori, T. (2001). Beclin-phosphatidylinositol 3-kinase complex functions at the trans-Golgi network. EMBO Rep. *2*, 330–335.

Klionsky, D.J., and Emr, S.D. (2000). Autophagy as a regulated pathway of cellular degradation. Science *290*, 1717–1721.

Knebelmann, B., Ananth, S., Cohen, H.T., and Sukhatme, V.P. (1998). Transforming growth factor alpha is a target for the von Hippel-Lindau tumor suppressor. Cancer Res. *58*, 226–231.

Kochl, R., Hu, X.W., Chan, E.Y., and Tooze, S.A. (2006). Microtubules facilitate autophagosome formation and fusion of autophagosomes with endosomes. Traffic *7*, 129–145.

Kondo, K., Kim, W.Y., Lechpammer, M., and Kaelin, W.G., Jr. (2003). Inhibition of HIF2alpha is sufficient to suppress pVHL-defective tumor growth. PLoS Biol. *1*, E83.

Kondo, Y., Kanzawa, T., Sawaya, R., and Kondo, S. (2005). The role of autophagy in cancer development and response to therapy. Nat. Rev. Cancer *5*, 726–734.

Lee, J.A., Beigneux, A., Ahmad, S.T., Young, S.G., and Gao, F.B. (2007). ESCRT-III dysfunction causes autophagosome accumulation and neurodegeneration. Curr. Biol. *17*, 1561–1567.

Lolkema, M.P., Gervais, M.L., Snijckers, C.M., Hill, R.P., Giles, R.H., Voest, E.E., and Ohh, M. (2005). Tumor suppression by the von Hippel-Lindau protein requires phosphorylation of the acidic domain. J. Biol. Chem. *280*, 22205–22211.

Mabjeesh, N.J., Escuin, D., LaVallee, T.M., Pribluda, V.S., Swartz, G.M., Johnson, M.S., Willard, M.T., Zhong, H., Simons, J.W., and Giannakakou, P. (2003). 2ME2 inhibits tumor growth and angiogenesis by disrupting microtubules and dysregulating HIF. Cancer Cell *3*, 363–375.

Mathew, R., Kongara, S., Beaudoin, B., Karp, C.M., Bray, K., Degenhardt, K., Chen, G., Jin, S., and White, E. (2007). Autophagy suppresses tumor progression by limiting chromosomal instability. Genes Dev. *21*, 1367–1381.

Mizushima, N., Yamamoto, A., Hatano, M., Kobayashi, Y., Kabeya, Y., Suzuki, K., Tokuhisa, T., Ohsumi, Y., and Yoshimori, T. (2001). Dissection of autophagosome formation using Apg5-deficient mouse embryonic stem cells. J. Cell Biol. *152*, 657–668.

Moeller, B.J., Dreher, M.R., Rabbani, Z.N., Schroeder, T., Cao, Y., Li, C.Y., and Dewhirst, M.W. (2005). Pleiotropic effects of HIF-1 blockade on tumor radiosensitivity. Cancer Cell *8*, 99–110.

Na, X., Duan, H.O., Messing, E.M., Schoen, S.R., Ryan, C.K., di Sant'Agnese, P.A., Golemis, E.A., and Wu, G. (2003). Identification of the RNA polymerase II subunit hsRPB7 as a novel target of the von Hippel-Lindau protein. EMBO J. *22*, 4249–4259.

Nazarko, T.Y., Farre, J.C., Polupanov, A.S., Sibirny, A.A., and Subramani, S. (2007). Autophagy-related pathways and specific role of sterol glucoside in yeasts. Autophagy *3*, 263–265.

Ogata, M., Hino, S., Saito, A., Morikawa, K., Kondo, S., Kanemoto, S., Murakami, T., Taniguchi, M., Tanii, I., Yoshinaga, K., et al. (2006). Autophagy is activated for cell survival after endoplasmic reticulum stress. Mol. Cell. Biol. *26*, 9220–9231.

Ohh, M., Yauch, R.L., Lonergan, K.M., Whaley, J.M., Stemmer-Rachamimov, A.O., Louis, D.N., Gavin, B.J., Kley, N., Kaelin, W.G., Jr., and Iliopoulos, O. (1998). The von Hippel-Lindau tumor suppressor protein is required for proper assembly of an extracellular fibronectin matrix. Mol. Cell *1*, 959–968.

Okuda, H., Saitoh, K., Hirai, S., Iwai, K., Takaki, Y., Baba, M., Minato, N., Ohno, S., and Shuin, T. (2001). The von Hippel-Lindau tumor suppressor protein mediates ubiquitination of activated atypical protein kinase C. J. Biol. Chem. *276*, 43611–43617.

Opipari, A.W., Jr., Tan, L., Boitano, A.E., Sorenson, D.R., Aurora, A., and Liu, J.R. (2004). Resveratrol-induced autophagocytosis in ovarian cancer cells. Cancer Res. *64*, 696–703.

Oya, M., Ohtsubo, M., Takayanagi, A., Tachibana, M., Shimizu, N., and Murai, M. (2001). Constitutive activation of nuclear factor-kappaB prevents TRAIL-induced apoptosis in renal cancer cells. Oncogene *20*, 3888–3896.

Patel, P.H., Chadalavada, R.S., Chaganti, R.S., and Motzer, R.J. (2006). Targeting von Hippel-Lindau pathway in renal cell carcinoma. Clin. Cancer Res. *12*, 7215–7220.

Perry, R.J., and Ridgway, N.D. (2006). Oxysterol-binding protein and vesicle-associated membrane protein-associated protein are required for sterol-dependent activation of the ceramide transport protein. Mol. Biol. Cell *17*, 2604–2616.

Qi, H., and Ohh, M. (2003). The von Hippel-Lindau tumor suppressor protein sensitizes renal cell carcinoma cells to tumor necrosis factor-induced cytotoxicity by suppressing the nuclear factor-kappaB-dependent antiapoptotic pathway. Cancer Res. *63*, 7076–7080.

Rapisarda, A., Uranchimeg, B., Scudiero, D.A., Selby, M., Sausville, E.A., Shoemaker, R.H., and Melillo, G. (2002). Identification of small molecule inhibitors of hypoxia-inducible factor 1 transcriptional activation pathway. Cancer Res. *62*, 4316–4324.

Smukste, I., Bhalala, O., Persico, M., and Stockwell, B.R. (2006). Using small molecules to overcome drug resistance induced by a viral oncogene. Cancer Cell *9*, 133–146.

Sosman, J.A., Puzanov, I., and Atkins, M.B. (2007). Opportunities and obstacles to combination targeted therapy in renal cell cancer. Clin. Cancer Res. *13*, 764s–769s.

Staller, P., Sulitkova, J., Lisztwan, J., Moch, H., Oakeley, E.J., and Krek, W. (2003). Chemokine receptor CXCR4 downregulated by von Hippel-Lindau tumour suppressor pVHL. Nature *425*, 307–311.

Sutphin, P.D., Chan, D.A., and Giaccia, A.J. (2004). Dead cells don't form tumors: HIF-dependent cytotoxins. Cell Cycle *3*, 160–163.

Takeuchi, H., Kondo, Y., Fujiwara, K., Kanzawa, T., Aoki, H., Mills, G.B., and Kondo, S. (2005). Synergistic augmentation of rapamycin-induced autophagy in malignant glioma cells by phosphatidylinositol 3-kinase/protein kinase B inhibitors. Cancer Res. *65*, 3336–3346.

Tanida, I., Tanida-Miyake, E., Komatsu, M., Ueno, T., and Kominami, E. (2002). Human Apg3p/Aut1p homologue is an authentic E2 enzyme for multiple substrates, GATE-16, GABARAP, and MAP-LC3, and facilitates the conjugation of hApg12p to hApg5p. J. Biol. Chem. *277*, 13739–13744.

Thomas, G.V., Tran, C., Mellinghoff, I.K., Welsbie, D.S., Chan, E., Fueger, B., Czernin, J., and Sawyers, C.L. (2006). Hypoxia-inducible factor determines sensitivity to inhibitors of mTOR in kidney cancer. Nat. Med. *12*, 122–127.

Yorikawa, C., Shibata, H., Waguri, S., Hatta, K., Horii, M., Katoh, K., Kobayashi, T., Uchiyama, Y., and Maki, M. (2005). Human CHMP6, a myristoylated ESCRT-III protein, interacts directly with an ESCRT-II component EAP20 and regulates endosomal cargo sorting. Biochem. J. *387*, 17–26.

Yorimitsu, T., Nair, U., Yang, Z., and Klionsky, D.J. (2006). Endoplasmic reticulum stress triggers autophagy. J. Biol. Chem. *281*, 30299–30304.

Young, A.R., Chan, E.Y., Hu, X.W., Kochl, R., Crawshaw, S.G., High, S., Hailey, D.W., Lippincott-Schwartz, J., and Tooze, S.A. (2006). Starvation and ULK1-dependent cycling of mammalian Atg9 between the TGN and endosomes. J. Cell Sci. *119*, 3888–3900.

Zimmer, M., Doucette, D., Siddiqui, N., and Iliopoulos, O. (2004). Inhibition of hypoxia-inducible factor is sufficient for growth suppression of VHL−/− tumors. Mol. Cancer Res. *2*, 89–95.